JACS
JOURNAL OF THE AMERICAN CHEMICAL SOCIETY

COMMUNICATION

pubs.acs.org/JACS

Dependence of Li_2FeSiO_4 Electrochemistry on Structure

Chutchamon Sirisopanaporn,[†,‡,∥] Christian Masquelier,[†,∥] Peter G. Bruce,[§,∥] A. Robert Armstrong,[§,∥] and Robert Dominko*[,‡,∥]

[†]LRCS, Université de Picardie Jules Verne, 33 Rue Saint-Leu, 80039 Amiens, France

[‡]National Institute of Chemistry, Hajdrihova 19, SI-1000 Ljubljana, Slovenia

[§]School of Chemistry, University of St. Andrews, North Haugh, St. Andrews, Fife KY16 9ST, Scotland

[∥]ALISTORE-ERI, 80039 Amiens Cedex, France

Supporting Information

ABSTRACT: Small differences in the FeO_4 arrangements (orientation, size, and distortion) do influence the equilibrium potential measured during the first oxidation of Fe^{2+} to Fe^{3+} in all polymorphs of Li_2FeSiO_4.

Lithium transition metal silicates, Li_2MSiO_4 (M = Fe, Mn, Co),[1] have attracted a lot of interest recently as positive electrodes for Li-ion batteries due to their potentially high theoretical capacities and to their rich crystal chemistry as they undergo complex polymorphism. Polymorphs of these "tetrahedral" structures can be classified into low- and high-temperature forms, which differ in the ordering/distribution of cations within tetrahedral sites of a hexagonal close-packed-based arrangement of oxygen.[2] Recent progress in the structure determination of Li_2MSiO_4 polymorphs[2] paves the way for a detailed study of the mechanisms of Li extraction/insertion from/into these silicates as a function of local and/or long-range order of cations. The achievements in the synthesis of electrochemically active Li_2FeSiO_4 (small, carbon-coated particles) prompted us to study in detail their electrochemical properties as a function of the crystal structure adopted.

We carefully prepared and used three polymorphs of Li_2FeSiO_4 with very high purity. A pristine powder had been obtained first under hydrothermal conditions[3] at 200 °C, labeled as LFS@200 and subsequently annealed at either 700 °C (LFS@700) or 900 °C (LFS@900) for 6 h and quenched to room temperature. Hydrothermal synthesis, experimental techniques used (X-ray diffraction, microscopy, electrochemical characterizations, Mössbauer spectroscopy, electrode preparations), and C-coating procedure are given in the Supporting Information.

The differences in the local environments of Fe^{2+} for between the three polymorphs are shown in Scheme 1. They differ in the interconnectivity of LiO_4 and SiO_4 tetrahedra and in their respective orientations along a given crystallographic direction. For all three polymorphs, only corner sharing occurs between FeO_4 and SiO_4 due to their strong discrepancy in O−O edge lengths. Each corner of a given FeO_4 tetrahedron, for all three polymorphs, is connected to two Li^+ and one Si^{4+} cation.

- In LFS@900 (*Pmnb* S.G.),[2d,e] a given FeO_4 tetrahedron shares two edges with LiO_4 tetrahedra
- In LFS@700 ($P2_1/n$ S.G.),[2a,d] only one edge is shared between FeO_4 and LiO_4
- In LFS@200 ($Pmn2_1$ S.G.),[1b] only corner sharing occurs

Scheme 1. Local Environments around FeO_4 Tetrahedra (In Green) in the Three Polymorphs of Li_2FeSiO_4 (LiO_4 in Gray, SiO_4 in Blue)

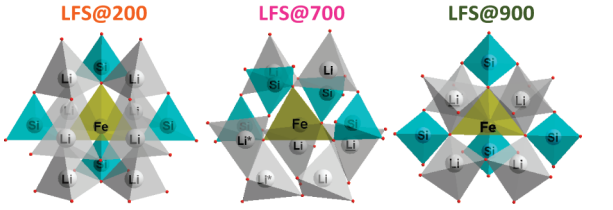

Table 1. Average Distances of Fe−O, Li−O, and Si−O Bonds and FeO_4 Distortion

	LFS@200	LFS@700	LFS@900
d_{avg} (Fe−O)/Å	2.076(3)	2.032(2)	2.026(1)
d_{avg} (Li−O)/Å	1.968(2)	1.970(1)	1.964(2)
d_{avg} (Si−O)/Å	1.636(2)	1.634(2)	1.656(4)
FeO_4 distortion[5] /Å^3	2.3×10^{-4}	9.9×10^{-4}	12.8×10^{-4}

As seen in Table 1, the differences in local environments around a given FeO_4 tetrahedron are immediately translated into varying degrees of distortion and average Fe−O bond lengths. Compared with usual distances in tetrahedral environments of oxides,[4] LFS@900 and LFS@700 show contraction of the average Fe−O distances so as to accommodate edge sharing with the slightly smaller LiO_4 tetrahedra. Importantly, shorter average Fe−O interatomic distances imply stronger (more covalent) Fe−O bonds, which should have a direct effect onto the redox potential of the Fe^{2+}/Fe^{3+} couple. Indeed, seminal work by Goodenough's group on polyanion structures (sulfates, tungstates, molybdates, phosphates)[6] demonstrated that a more ionic Fe−O bond (hence longer) resulted in lowering the energy of the antibonding states and thus increasing the voltage vs Li^+/Li^0 at which oxidation of Fe^{2+} into Fe^{3+} would take place. This is particularly true for $LiFePO_4$, which shows edge sharing between FeO_6 and PO_4 and displays[6b,c] the highest value of voltage vs Li for iron in phosphates: 3.42 V vs Li^+/Li^0.

Received: October 28, 2010
Published: December 30, 2010

dx.doi.org/10.1021/ja109695r | J. Am. Chem. Soc. 2011, 133, 1263–1265

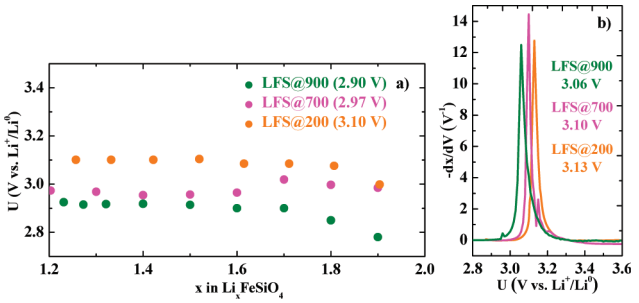

Figure 1. (a) Equilibrium potentials measured from GITT. (b) Derivative plots obtained from PITT in the first oxidation of three polymorphs.

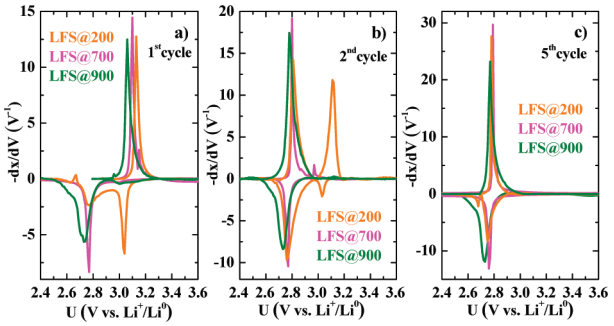

Figure 2. Derivative plots obtained from PITT measurements in the first, second, and fifth cycles for all three polymorphs.

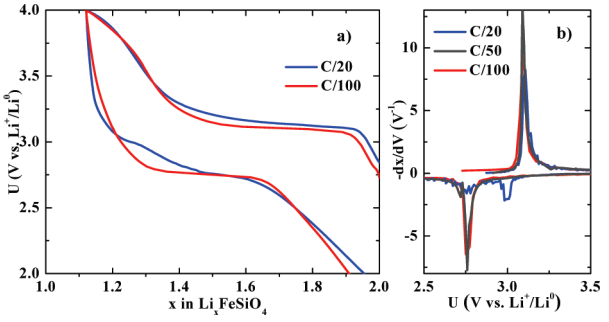

Figure 3. (a) Galvanostatic curves in the first cycle. (b) Derivative plots of galvanostatic curves in the first cycle of LFS@700 polymorph.

Three well-defined (crystallographically) samples (LFS@200, LFS@700, and LFS@900) were used for electrochemical characterization in order to investigate the influence of crystal structures on their electrochemical properties. Within the aim to homogenize the particle size and to improve electron contacts in the non-carbon-coated samples, we performed ball milling with Ketjen black under an argon atmosphere. Typical particle size used in our study was between 60 and 150 nm. Rietveld refinements of both pristine materials and electrode composites have been performed so as to confirm the crystal structures of the materials used (Figures S1 and S3 and Tables S1, S2, S4, and S5 in Supporting Information).

The precise positions of the Fe^{2+}/Fe^{3+} redox couple vs Li^+/Li^0 for each polymorph were carefully investigated using GITT and PITT techniques, which enable measurements close to the equilibrium potential (see Supporting Information). The use of GITT clarifies the difference in the first oxidation potential among the three polymorphs, as shown in Figure 1a. The lowest potential was observed in the case of LFS@900 (2.90 V vs Li^+/Li^0), while the highest was that of LFS@200 (3.10 V vs Li^+/Li^0). The equilibrium potential of LFS@700 was close to 3.00 V vs Li^+/Li^0. PITT measurements have been performed to substantiate the observed differences in the equilibrium potentials among the various polymorphs. The results are in agreement with those measured from GITT; the first oxidation potential (vs Li^+/Li^0) increases from LFS@900 to LFS@200, as shown in Figure 1b. One may note that the potentials measured from GITT are lower than those obtained from PITT. This could be explained by the activation energy needed for initial lithium extraction. Importantly, the coherence of the results obtained from both electrochemical techniques has confirmed the influence of the crystallographic structures on the position of the Fe^{2+}/Fe^{3+} redox potential in Li_2FeSiO_4. In other words, shorter average Fe−O bond lengths (i.e., higher covalency of the Fe−O bonds) and higher degree of distortion of the FeO_4 tetrahedra result in higher Fe^{2+}/Fe^{3+} redox energy (hence smaller voltage difference with Li^+/Li^0) through the inductive effect.

The use of PITT technique has pointed out another peculiarity of the rich polymorphism of Li_2FeSiO_4. The electrochemical measurements of the three polymorphs, besides showing the "classical" irreversible change of cell voltage from ∼3.0 to ∼2.8 V between the first and subsequent charges,[7] highlight significant differences in the kinetics associated with these transformations.

As seen in Figure 2a−c, the high-temperature polymorphs (LFS@900 and LFS@700), with higher degree of "disorder" in terms of cation connectivity, are prone to transform into the thermodynamic favorable phase faster than the low-temperature (LFS@200) one. The first discharge of LFS@900 and LFS@700 occurs at a reduction potential of ∼2.76 V vs Li^+/Li^0, while two reduction peaks at ∼2.76 and ∼3.04 V were observed in the case of LFS@200. The potential around 3 V is associated with the remaining initial Li_2FeSiO_4 phase, whereas the new Li-poor phase, originated upon first oxidation, shows the reduction potential at ∼2.76 V. Moreover, an oxidation peak at 3.13 V could be observed in the second cycle of LFS@200, indicating a significant amount of initial LFS@200 phase (Figure 2b). Subsequently the irreversible transformation of LFS@200 is completed in the fifth cycle, while only first oxidation is needed for the structural rearrangement of LFS@700 and LFS@900.

Using conventional galvanostatic measurements, we observed that the applied current density is also important to the phase transformation kinetics. For instance, as seen in Figure 3, the residual of the initial LFS@700 phase could be observed only for the battery which cycled with high current density. Hence, not only the crystal structure but also the current density used in the experiment influence the kinetics of thermodynamic stabilization. Similar effects have been observed by varying the temperature at which the electrochemical tests were performed.

In this Communication, we used three very well-defined crystallographically pure Li_2FeSiO_4 samples crystallized in *Pmnb* (LFS@900), $P2_1/n$ (LFS@700), and $Pmn2_1$ (LFS@200) space groups. Variations in the FeO_4 arrangements (orientation, size, and distortion) influence the equilibrium potential measured during the first oxidation of Fe^{2+} into Fe^{3+} in all polymorphs. The shorter (stronger) Fe−O bonds result in the higher splitting energy between bonding and antibonding states, and thus lowering the Fe^{2+}/Fe^{3+} redox potential vs Li^+/Li^0. More surprisingly, phase transformation kinetics of Li_2FeSiO_4 upon cycling has structural, cycling rate, and temperature dependence.

dx.doi.org/10.1021/ja109695r |*J. Am. Chem. Soc.* 2011, 133, 1263–1265

■ ASSOCIATED CONTENT

Supporting Information. Experimental part, refined X-ray diffraction patterns, tables with crystallographic data, and SEM micrographs. This material is available free of charge via the Internet at http://pubs.acs.org.

■ AUTHOR INFORMATION

Corresponding Author
Robert.Dominko@ki.si

■ ACKNOWLEDGMENT

The Ministère de l'Enseignement Supérieur et de la Recherche, France, is acknowledged for supporting C.S. through an international PhD student scholarship.

■ REFERENCES

(1) (a) Nyten, A.; Abouimrane, A.; Armand, M.; Gustafsson, T.; Thomas, J. O. *Electrochem. Commun.* **2005,** *7*, 156–160. (b) Dominko, R.; Bele, M.; Gaberscek, M.; Meden, A.; Remskar, M.; Jamnik, J. *Electrochem. Commun.* **2006,** *8*, 217–222. (c) Lyness, C.; Delobel, B.; Armstrong, A. R.; Bruce, P. G. *Chem. Commun.* **2007,** 4890–4892.

(2) (a) Nishimura, S. I.; Hayase, S.; Kanno, R.; Yashima, M.; Nakayama, N.; Yamada, A. *J. Am. Chem. Soc.* **2008,** *130*, 13212–13213. (b) Politaev, V. V.; Petrenko, A. A.; Nalbandyan, V. B.; Medvedev, B. S.; Shvetsova, E. S. *J. Solid State Chem.* **2007,** *180*, 1045. (c) Mali, G.; Meden, A.; Dominko, R. *Chem. Commun.* **2010,** *43*, 3306. (d) Boulineau, A.; Sirisopanaporn, C.; Dominko, R.; Armstrong, A. R.; Bruce, P. G.; Masquelier, C. *Dalton Trans.* **2010,** *39*, 6310. (e) Sirisopanaporn, C.; Boulineau, A.; Armstrong, A. R.; Bruce, P. G.; Hanzel, D.; Budic, B.; Dominko, R.; Masquelier, C. *Inorg. Chem.* **2010,** *47*, 7446.

(3) (a) Dominko, R.; Conte, D. E.; Hanzel, D.; Gaberscek, M.; Jamnik, J. *J. Power Sources* **2007,** *178*, 842. (b) Nadherna, M.; Dominko, R.; Hanzel, D.; Reiter, J.; Gaberscek, M. *J. Electrochem. Soc.* **2009,** *156*, A619.

(4) Shannon, R. D.; Prewitt, C. T. *Acta Crystallogr.* **1969,** *B25*, 925.

(5) Rodriguez-Carvajal, J. *Phys. Rev. Lett.* **1998,** *21*, 4660.

(6) (a) Manthiram, A.; Goodenough, J. B. *Power Sources* **1989,** *26*, 403. (b) Padhi, A. K.; Nanjundaswamy, K. S.; Masquelier, C.; Goodenough, J. B. *J. Electrochem. Soc.* **1997,** *144*, 2581–2588. (c) Padhi, A. K.; Nanjundaswamy, K. S.; Masquelier, C.; Okada, S.; Goodenough, J. B. *J. Electrochem. Soc.* **1997,** *144*, 1609–1613.

(7) Nyten, A.; Kamali, S.; Haggstrom, L.; Gustafsson, T.; Thomas, J. O. *J. Mater. Chem.* **2006,** *16*, 2266.